Biogeosciences Discuss., doi:10.5194/bg-2016-284, 2016
Manuscript under review for journal Biogeosciences
Published: 14 July 2016

Quantifying Soil Carbon Accumulation in Alaskan Terrestrial Ecosystems during the Last 15,000 Years

Sirui Wang[1], Qianlai Zhuang[1,2*], Zicheng Yu[3]

[1]Department of Earth, Atmospheric, and Planetary Sciences, Purdue University, West Lafayette, Indiana, 47907

[2]Department of Agronomy, Purdue University, West Lafayette, IN 47907

[3]Department of Earth and Environmental Sciences, Lehigh University, Bethlehem, PA 18015

Correspondence to: qzhuang@purdue.edu

Abstract: Northern high latitudes contain large amounts of soil organic carbon (SOC), in which Alaskan terrestrial ecosystems account for a substantial proportion. In this study, the SOC accumulation in Alaskan terrestrial ecosystems over the last 15,000 years was simulated using a process-based biogeochemistry model for both peatland and non-peatland terrestrial ecosystems. Comparable with the previous estimates of 25-70 Pg C in peatland and 13-22 Pg C in non-peatland soils within 1-m depth in Alaska, our model estimated a total SOC of 36-63 Pg C at present, including 27-48 Pg C in peatland soils and 9-15 Pg C in non-peatland soils. Vegetation stored only 2.5-3.7 Pg C in Alaska currently with 0.3-0.6 Pg C in peatlands and 2.2-3.1 Pg C in non-peatlands. The simulated average rate of peat C sequestration was 2.3 Tg C yr^{-1} with a peak value of 5.1 Tg C yr^{-1} during the Holocene Thermal Maximum (HTM) in the early Holocene, four folds higher than the average rate of 1.4 Tg C yr^{-1} over the rest of the Holocene. The SOC accumulation slowed down, or even ceased, during the neoglacial climate cooling after the mid-Holocene, but accumulation increased again in the 20th century. The model-estimated peat depths ranged from 1.1 to 2.7 m, similar to the field-based estimate of 2.29 m for the region. We found that the changes in vegetation types and their distributions due to climate change were the main factors determining the spatial variations of SOC accumulation during different time periods. Warmer summer temperature and stronger radiation seasonality, along with higher precipitation in the HTM and the 20th century might have resulted in the extensive peatland expansion and carbon accumulation, implying that soil C accumulation would continue under future warming conditions.

Keywords: Carbon, Peatlands, Alaska, Modelling, Climate

Biogeosciences Discuss., doi:10.5194/bg-2016-284, 2016
Manuscript under review for journal Biogeosciences
Published: 14 July 2016

1. Introduction

Global surface air temperature has been increasing since the middle of the 19th century (Jones and Mogberg, 2003; Manabe and Wetherald, 1980, 1986). Since 1970, the warming trend has accelerated at a rate of 0.35 ℃ per decade in northern high latitudes (Euskirchen et al., 2007; McGuire et al., 2009). It is predicted that the warming will continue in the next 100 years (Arctic Climate Impact Assessment 2005; Intergovernmental Panel on Climate Change (IPCC), 2013, 2014). The land surface in northern high latitudes (>45° N) occupies 22% of the global surface and stores over 40% of the global soil organic carbon (SOC) (McGuire et al., 1995; Melillo et al., 1995; McGuire and Hobbie, 1997). Specifically, the northern high latitudes were estimated to store 200-600 Pg C (1 Pg C = 10^{15} g C) in peatland soils depending on the depth considered (Gorham, 1990, 1991; Yu, 2012), 750 Pg C in non-peatland soils (within 3 m) (Schuur et al., 2008; Tarnocai et al., 2009; Hugelius et al., 2014), and additional 400 Pg C in frozen loess deposits of Siberia (Zimov et al., 2006a). Peatland area is around 40 million hectares in Alaska compared with total 350 million hectares in northern high-latitude regions (Kivinen and Pakarinen, 1981). Alaskan peatlands account for the most vast peatland area in the USA and cover at least 8% of total land area (Bridgham et al., 2006). To date, the regional soil C and its responses to the climate change are still with large uncertainty (McGuire et al., 2009; Loisel et al., 2014).

The warming climate could increase C input to soils as litters through stimulating plant net primary production (NPP) (Loisel et al., 2012). However, it can also decrease the SOC by increasing soil respiration (Yu et al., 2009). Warming can also draw down the water table in peatlands by increasing evapotranspiration, resulting in a higher decomposition rate as the aerobic respiration has a higher rate than anaerobic respiration in general (Hobbie et al., 2000).

SOC accumulates where the rate of soil C input is higher than decomposition. The variation of climate may switch the role of soils between a C sink and a C source (Davidson and Janssens, 2006; Davidson et al., 2000; Jobbagy and Jackson, 2000). Unfortunately, due to the data gaps of field-measurement and uncertainties in estimating regional C stock (Yu, 2012), with limited understanding of both peatlands and non-peatlands and their responses to climate change, there is no consensus on the sink and source activities of these ecosystems (Frolking et al., 2011; Belyea, 2009; McGuire et al., 2009).

To date, both observation and model simulation studies have been applied to understand the long-term peat C accumulation in northern high latitudes. Most field estimations are based on series of peat-core samples (Turunen et al., 2002; Roulet et al., 2007; Yu et al., 2009; Tarnocai et al., 2009). However, those core analyses may not be adequate for estimating the regional C accumulation due to their limited spatial coverage. Model simulations have also been carried out. For instance, Frolking et al. (2010) developed a peatland model considering the effects of plant community, hydrological dynamics and peat properties on SOC accumulation. The simulated results were compared with peat-core data. They further analyzed the contributions of different plant functional types (PFTs) to the peat C accumulation. However, this 1-D model has not been used in large spatial-scale simulations by considering other environmental factors (e.g., temperature, vapor pressure, and radiation). In contrast, Spahni et al. (2013) used a dynamic global vegetation and land surface process model (LPX), based on LPJ (Sitch et al., 2003), imbedded with a peatland module, which considered the nitrogen feedback on plant productivity (Xu-Ri and Prentice, 2008) and plant biogeography, to simulate the SOC accumulation rates of northern peatlands. However, these models have not been evaluated with respect to their simulations of soil moisture, water table depth, methane fluxes, and carbon fluxes presumably

Biogeosciences Discuss., doi:10.5194/bg-2016-284, 2016
Manuscript under review for journal Biogeosciences
Published: 14 July 2016

due to relatively simple model structures, especially in terms of ecosystem processes (Stocker et al., 2011, 2014; Kleinen et al., 2010). Furthermore, climatic effects on SOC were not fully explained. The Terrestrial Ecosystem Model (TEM) has been applied to study C and nitrogen pools and fluxes in the Arctic (Zhuang et al., 2001, 2002, 2003, 2015; He et al., 2014). However, the model has not been calibrated and evaluated with peat-core C data, and has not been applied to investigate the peatland C dynamics. Building upon these efforts, recently we fully evaluated the peatland version of TEM (P-TEM) including modules of hydrology (HM), soil thermal (STM), C and nitrogen dynamics (CNDM) for both upland and peatland ecosystems (Wang et al., 2016).

Here we used the peatland-core data for various peatland ecosystems to parameterize and test P-TEM (Figure 1). The model was then used to quantify soil C accumulation of both peatland and non-peatland ecosystems across the Alaskan landscape since the last deglaciation. This study is among the first to examine the current peatlands and non-peatlands C distributions and peat depths in various ecosystems at the regional scale.

2. Methods

2.1 Model Description

In P-TEM, peatland soil organic C (SOC) accumulation is determined by the difference between the net primary production (NPP) and aerobic and anaerobic decompostion. Peatlands accumulate C where NPP is greater than decomposition, resulting in positive net ecosystem production (NEP):

Biogeosciences Discuss., doi:10.5194/bg-2016-284, 2016
Manuscript under review for journal Biogeosciences
Published: 14 July 2016

$$NEP = NPP - R_H - R_{CH_4} - R_{CWM} - R_{CM} - R_{COM} \quad (1)$$

P-TEM was develoepd based on the Terrestrial Ecosystem Model (TEM) at a monthly step (Zhuang et al., 2003; 2015). It explicitly considers the process of aerobic decomposition (R_H) related to the variability of water-table depth; net methane emission after methane oxidation (R_{CH_4}); CO_2 emission due to methane oxidation (R_{CWM}) (Zhuang et al., 2015); CO_2 release accompanied with the methanogenesis (R_{CM}) (Tang et al., 2010; Conrad, 1999); and CO_2 release from other anaerobic processes (R_{COM}, e.g., fermentation, terminal electron acceptor (TEA) reduction) (Keller and Bridgham, 2007; Keller and Takagi, 2013). For upland soils, we only considered the heterotrohic respiration under aerobic condition (Raich, 1991). For detailed model description see Supplement.

We model peatland soils as a two-layer system for hydrological module (HM) while keeping the three-layer system for upland soils (Zhuang et al., 2002). The soil layers above the lowest water table position are divided into: (1) moss (or litter) organic layer (0-10 cm); and (2) humic organic layer (10-30 cm) (Wang et al., 2016). Based on the total amount of water content within those two unsaturated layers, the actual water table depth (WTD) is estimated. The water content at each 1 cm above the water table can be then determined after solving the water balance equations (Zhuang et al., 2004).

In the STM module, the soil vertical profile is divided into four layers: (1) snowpack in winter, (2) moss (or litter) organic layer, (3) upper and (4) lower humic organic soil (Wang et al., 2016). Each of these soil layers is characterized with a distinct soil thermal conductivity and heat capacity. We used the observed water contents at the particular sites to drive the STM (Zhuang et al., 2001).

Biogeosciences Discuss., doi:10.5194/bg-2016-284, 2016
Manuscript under review for journal Biogeosciences
Published: 14 July 2016

The methane dynamics module (MDM) (Zhuang et al., 2004) considers the processes of methanogenesis, methanotrophy, and the transportation pathways including: (1) diffusion through the soil profile; (2) plant-aided transportation; and (3) ebullition. The soil temperatures calculated from STM, after interpolation into 1-cm sub-layers, are input to the MDM. The water table depth and soil water content in the unsaturated zone for methane production and emission are obtained from HM, and the net primary production (NPP) is calculated from the CNDM. Soil-water pH is prescribed from observed data and the root distribution determines the redox potential (Zhuang et al., 2004).

2.2 Model Parameterization

We have parameterized the key parameters of the individual modules including HM, STM, and MDM (Wang et al., 2016). The parameters in CNDM for upland soils and vegetation have been optimized in the previous studies (Zhuang et al 2002, 2003; Tang and Zhuang 2008). The parameters for peatland soils in P-TEM were parameterized using a moderate rich *Sphagnum* spp. open fen (APEXCON) and a *Sphagnum*-black spruce (*Picea mariana*) bog (APEXPER) (Table 3). Both are located in the Alaskan Peatland Experiment site (APEX) study area, where *Picea mariana* is the only tree species above breast height in APEXPER. Three water table position manipulations were established in APEX including a control, a lowered, and a raised water table plots (Chivers et al., 2009; Turetsky et al., 2008; Kane et al., 2010; Churchill et al., 2011). There were also several internal collapse scars that formed with thaw of surface permafrost, including a non-, an old, and a new collapse plots. APEXCON represents the control manipulation and APEXPER represents the non-collapse plot. The annual NPP and aboveground biomass at both sites have been measured in 2009. There were no belowground observations; however, at a Canadian peatland, Mer Bleue, which includes *Sphagnum* spp. dominated bog (dominated by shrubs and *Sphagnum*) and pool fen (dominated by sedges and herbs and *Sphagnum*). Assuming the belowground biomass in APEXCON and APEXPER was close to that in Mer Bleue, we used the belowground biomass at Mer Bleue to represent the missing observations at both sites (Table 4). We conducted a set of 100,000 Monte Carlo ensemble simulations for each site-level calibration, and parameters with the highest mode in posterior distribution were selected (Tang and Zhuang, 2008, 2009).

2.3 Regional Vegetation Data

The Alaskan C stock was simulated through the Holocene where the vegetation biome maps were reconstructed at four time periods: a time period encompassing a millennial-scale warming event during the last deglaciation known as the BØlling-AllerØd at 15-11 ka (1 ka = 1000 cal yr Before Present), HTM during the early Holocene at 11-10 and 10-9 ka as well as the mid- (9-5 ka) and late- Holocene (9 ka-1900 AD) (He et al., 2014). We used the modern vegetation distribution for the simulation during the period 1900-2000 AD (Figure 2). We assumed that the vegetation distribution remained static within each corresponding time period. Five vegetation types were classified as upland vegetation: boreal deciduous broadleaf forest, boreal evergreen needleleaf and mixed forest, alpine tundra, wet tundra; and barren (Table 1). Mountain ranges and large water bodies were delineated as 'Barren' and data could not be interpolated across them. By using the same vegetation distribution map, we reclassified the upland vegetation into two peatland vegetation types: *Sphagnum* spp. poor fens (SP) generated from tundra ecosystems, and *Sphagnum* spp-black spruce (*Picea mariana*) bog/ peatland (SBP) generated from forest ecosystems (Table 1), both of which dominate the major area of Alaskan peatlands. We used both the upland and peatland vegetation types to simulate the C dynamics in Alaska.

Upland and peatland distribution for each grid cell was determined using the wetland inundation data extracted from the NASA/ GISS global natural wetland dataset (Matthews and Fung, 1987). The resolution was resampled to 0.5° × 0.5° from 1° × 1°. We postulated that, given the same topography of Alaska during the Holocene, it was reasonable to assume that the wetland distribution can be represented by modern inundation map. The inundation fraction was assumed to be the same within each grid through time and the land grids not covered by expanded peatland yet were assumed as uplands. We calculated the total area of modern Alaskan peatlands to be 302,410 km^2, which was within the range from 132,000 km^2 (Bridgham et al., 2006) to 596,000 km^2 (Kivinen and Pakarinen, 1991). The soil water pH data were extracted from Carter and Scholes (2000), and the elevation data were derived from Shuttle Radar Topography Mission and were resampled to 0.5° × 0.5° spatial resolution.

2.4 Climate Data

Climate data were downscaled and bias-corrected from ECBilt-CLIO model output (Timm and Timmermann, 2007; He et al., 2014). Climate fields include monthly precipitation, monthly air temperature, monthly net incoming solar radiation, and monthly vapor pressure (2.5° × 2.5°). We used the same time-dependent forcing atmospheric carbon dioxide concentration data for model input as were used in ECBilt-CLIO transient simulations from the Taylor Dome (Timm and Timmermann, 2007). The historical climate data used for the simulation through the 20th century are monthly CRU2.0 data.

The mean annual net incoming solar radiation (NIRR) was 78 ± 4.8 W m^{-2} before the HTM (15-11 ka). It showed an increase at the early HTM (11-10 ka), reaching 83.6 ± 4.5 W m^{-2} and continueed to increase to 84 ± 4.7 W m^{-2} at the late HTM (10-9 ka). NIRR decreased after

Biogeosciences Discuss., doi:10.5194/bg-2016-284, 2016
Manuscript under review for journal Biogeosciences
Published: 14 July 2016

the HTM through the entire mid-Holocene (9-5 ka) to a minimum of 79$\pm$5 W m^{-2} at the end of the Holocene. It became higher from 1900 to 2000 AD, with annual mean 82$\pm$5.1 W m^{-2} (Figure 3b). The mean annual air temperature showed a similar pattern as it rose from -7$\pm$1.8 ℃ to -5$\pm$1.6 ℃ at the early HTM and reached -4.7$\pm$1.5 ℃ at the late HTM, indicating a warmer-than-present climate. There was also a temperature decrease when HTM ended through the rest of the Holocene and the temperature increased again from 1900 AD to -5.8$\pm$1.5 ℃, presumably due to the global warming (Figure 3d). Total annual precipitation increased from 306$\pm$40 mm to 369$\pm$25 mm at the end of the HTM, suggesting an overall wet climate. A dryer condition occurred from the mid-Holocene and became driest in the late-Holocene (5 ka-1900 AD) (Figure 3f). The monthly values of NIRR followed the same pattern as annual means, except during the winter. The maximum summer radiation occurred during the late-HTM, leading to the highest radiation seasonality. Large seasonality also appeared in the 20th century, however, lower than that during the HTM (Figure 3a). Temperature seasonality followed the trend of annual temperature. The days of year with temperature above 0 ℃ increased 10-15 days at the HTM compared with that before the HTM, suggesting a longer growing season (Figure 3c). Precipitations were highest during the summer (July-September) in each time period and lowest during the winter and early spring (December-April). The periods at 15-11ka and in the late-Holocene exhibited less overall, especially summer precipitations than at the HTM. During the 20th century, there was less winter precipitation but it was compensated by a higher summer precipitation compared with the late-Holocene (Figure 3e). The orbital induced maximum seasonality of insolation and the warmest climate during the HTM as described in Huybers et al. (2006) and Yu et al. (2010) corresponded well to the simulated trends of air temperature.

Biogeosciences Discuss., doi:10.5194/bg-2016-284, 2016
Manuscript under review for journal Biogeosciences
Published: 14 July 2016

2.5 Data of Peatland Basal Ages

We conducted the simulation from 15 to 5 ka for an Alaskan peatland assuming it started to accumulate C since 15 ka. However, assuming that peatlands in all grids had the same basal age (15 ka) could overestimate the total peat SOC accumulation. Therefore we used the observed basal ages of peat samples from Gorham et al. (2012) and categorized them into different time periods (Figure 2). We found that during each period, the spatial distribution of peatland basal ages was similar to that of the vegetation types (e.g., peatland initiation points were mainly located where was dominated by alpine tundra at south, northwestern, and southeastern coast during 15-11 ka). We thus used the vegetation types to estimate the peatland basal ages at regional scales (Table 2).

2.6 Simulations and Sensitivity Test

To verify the model ability to simulate the peat C accumulation rates in the past 15,000 years, we conducted a simulation using pixels located on the Kenai Peninsula from 15 to 5 ka after model parameterization. We compared the model simulation results with the peat-core data from four peatlands on the Kenai Peninsula, Alaska (Jones and Yu, 2010; Yu et al., 2010) (see Wang et al. (2016) for detail). The observed data include the peat depth, bulk density of both organic and inorganic matters at 1-cm interval, and age determinations. The simulated C accumulation rates represent the actual ("true") rates at different times in the past. However, the calculated accumulation rates from peat cores are considered as "apparent" accumulation rates, as peat would continue to decompose since the time of formation until present when the measurement was made (Yu, 2012). To facilitate comparison between simulated and observed accumulation rates, we converted the simulated "true" accumulation rates to "apparent" rates,

Biogeosciences Discuss., doi:10.5194/bg-2016-284, 2016
Manuscript under review for journal Biogeosciences
Published: 14 July 2016

following the approach by Spahni et al. (2013). That is, we summed the annual net C accumulation over each 500-year interval and deducted the total amount of C decomposition from that time period, then dividing by 500 years.

For the study region, we conducted a transient simulation using continuous monthly meteorology data (Figure 2) from 15 ka to 2000 AD. Five maps (Figure 3) were used to represent the vegetation distributions of Alaska and were assumed to be static during each time period (e.g., 15-11 ka, 11-10 ka, 10-9 ka, 9 ka-1900 AD, and 1900-2000 AD). The simulation was firstly conducted assuming all grid cells were taken up by upland vegetation to get the upland soil C spatial distributions during different time periods. We then conducted the second simulation assuming all grid cells were dominated by peatland vegetation by merging upland types into peatland types following Table 1 to obtain the distributions of peat SOC accumulation. We used the inundation fraction map to extract both uplands and peatlands from each grid and estimated the corresponding SOC stocks within each grid, which were then summed up to represent the Alaskan SOC stock.

We conducted a sensitivity test to evaluate the responses of NPP, SOC decomposition rates (aerobic plus anaerobic respiration), and net SOC balance to the climate variables. Simulations under three scenarios were conducted to test the temperature effect. We used the original forcing data as the standard scenario and the warmer (monthly temperature +5℃) and cooler (−5℃) as other two while keeping the rest forcing data unchanged. Similarly, we used the original forcing data as the standard scenario and the wetter (monthly precipitation +10 mm) and drier (−10 mm) to test the effect from precipitation. To further study if vegetation distribution has stronger effects on SOC sequestration than climate in Alaska, we simply replaced SBP with SP and simultaneously replaced the upland forests with tundra at the beginning of 15 ka. We also conducted the simulation under "warmer" and "wetter" conditions described before while keeping the vegetation distribution unchanged.

3. Results

3.1 Simulated Peatland Carbon Accumulation Rates at Site Level

Our paleo simulation showed a large peak of peat C accumulation rates at 11-9 ka during the HTM (Figure 4). The simulated "true" and "apparent" rates captured this primary feature in peat-core data at almost all sites (Jones and Yu, 2010). The simulated magnitude of this peak was similar to observations at No Name Creek and Horse Trail Fen, but overestimated at Kenai Gasfield and Swanson Fen at 10-9 ka (late-HTM). The secondary peak of C accumulation rates appeared at 6-5 ka in the mid-Holocene. The simulation successfully estimated both peaks at Swanson Fen, No Name Creek, and Kenai Gasfield, but with overestimated magnitude at Swanson Fen. The comparison between simulation and observation using averages in 500-year bins revealed a high correlation ($R^2 = 0.90, 0.88,$ and 0.39), especially at No Name Creek and Horse Trail Fen. The simulated SOC accumulation rates corresponded well to the synthesis curves at four sites (Figure 4b).

3.2 Vegetation Carbon Storage

Model simulations showed an overall low mean annual vegetation C storage before the HTM (15-11 ka) (Figure 5a), paralleled to the relatively low annual NPP (Figure 5b). The *Sphagnum*-dominated peatland represented the lowest vegetation C storage (2.5 kg $\mathrm{C\ m^{-2}}$), much lower than the *Sphagnum*-black spruce peatland (1 kg $\mathrm{C\ m^{-2}}$). Upland vegetation showed a generally higher C storage, with the highest amount of C stored in boreal evergreen needleleaf forests (2 kg $\mathrm{C\ m^{-2}}$). The upland forests also showed a higher rate of annual NPP (0.31-0.35

Biogeosciences Discuss., doi:10.5194/bg-2016-284, 2016
Manuscript under review for journal Biogeosciences
Published: 14 July 2016

kg C $m^{-2}yr^{-1}$). C storage of alpine and moist tundra was higher than peatlands, while the annual NPP were lower (0.08-0.1 kg C $m^{-2}yr^{-1}$). Higher NPP were shown in almost all vegetation types during the early Holocene. There were no significant changes of vegetation C storage in peatlands and tundra compared with boreal forests. All vegetation showed a higher NPP and vegetation C during the late-HTM. Mean annual vegetation C exceeded 0.5 g C m^{-2} and 1.3 g C m^{-2} for *Sphagnum* and black spruce peatlands. Evergreen forest stored over 4.7 kg C m^{-2}. During the mid-Holocene, almost all vegetation types represented a decrease in both NPP and vegetation C. The plant productivity along with the vegetation C began to slightly increase at late-Holocene and became stable, possibly resulted from the rising temperature.

Approximately 2 Pg C was stored in both upland and peatland vegetation in Alaska before the HTM (Figure 6). Upland moist tundra accounted for the most amount of C due to its large area. At the early HTM, evergreen needleleaf forest area became the largest, and about 1.9 Pg C was stored in boreal forests. More C was stored in black spruce peatland also because of the forest formation. Boreal forest accounted for 3.5 Pg C at the late HTM. Decrease of vegetation C occurred at mid-Holocene. The simulation through the Holocene to present indicated that the lowest amount C was stored in vegetation before the HTM, while vegetation assimilated the largest amount of C during the late-Holocene. We estimated a total 2.9 Pg C stored in modern Alaskan vegetation, with 0.4 Pg in peatlands and 2.5 Pg in non-peatlands. The uncertainties of the parameters during the model calibration (Table 4) resulted in a range of 0.3-0.6 Pg C and 2.2-3.1 Pg C in peatlands and non-peatlands, respectively.

Biogeosciences Discuss., doi:10.5194/bg-2016-284, 2016
Manuscript under review for journal Biogeosciences
Published: 14 July 2016

3.3 Soil Carbon Stocks

Carbon storage in Alaskan non-peatland soils varied spatially (Figure 7). Generally, deciduous broadleaf forests had a higher SOC (8-13 kg $\mathrm{C\ m^{-2}}$) than evergreen needleleaf forests (3-8 kg $\mathrm{C\ m^{-2}}$), while moist tundra had the highest SOC (12-25 kg $\mathrm{C\ m^{-2}}$). The SOC showed an overall increase in both boreal forests and moist tundra during the early-HTM (11-10 ka) (Figures 7a, b). With the continued expansion of the boreal forests during the late-HTM (10-9 ka) (Figure 4c), the spots of low SOC concentration were widely spread (Figure 7c). During the mid- (9-5 ka) and late-Holocene (5 ka-1900 AD), although the wet tundra took back the most area, the SOC decreased (Figure 7d) presumably due to the cooler and drier conditions, which was consistent with the decline in mean annual NPP and vegetation C (Figure 5). An increase occurred again in the last century with mean SOC comparable to the late-HTM (Figure 7f). An average of 3.1 Pg C was simulated before the HTM (Figure 8). The SOC increased sharply during the early-HTM (to 11.5 Pg C) across Alaska and slightly decreased to 9 Pg C at the end of HTM. There was little variation during the mid- and late-Holocene (10.7 Pg C) and the amount increased to 11.2 Pg C at the end of the 20th century. Due to model parameterization (Table 4), the regional soil C estimates ranged from 9 to 15 Pg C at present.

The peatland SOC showed a different pattern compared to upland soils. Peatlands started to accumulate C at 15 ka mainly in northwestern, southeastern, and south coastal regions of Alaska (Figure 9a). Much less C (<10 kg $\mathrm{C\ m^{-2}}$) was accumulated in the southeastern coast in comparison to other coastal parts (>15 kg $\mathrm{C\ m^{-2}}$). Initially, only *Sphagnum* open peatland (SP) existed, with no *Sphagnum*-black spruce forested peatland (SBP). At the beginning of the HTM, there was a peatland area of ~$4.5\times 10^5\ \mathrm{km^2}$ (Figure 10). During the early-HTM, the SP formed in the north coast and the SBP rapidly expanded in south coast and east central regions, becoming the dominant peatland type in Alaska (Figure 9b). Meanwhile the peatlands area increased to ~13×10^5 km^2 (Figure 10). The SBP continued to expand to the central Alaska during the late-HTM (Figure 9c). Although peatlands continued to form towards west in the mid-Holocene (Figures 9d, 10), some areas that were dominated by SBP in interior Alaska stopped accumulating SOC. By the end of the mid-Holocene, almost all the peatlands have formed (Figure 10) and some grids showed negative accumulation in the late-Holocene (Figure 9e). However, as the global warming began in the 20th century, SOC accumulation increased rapidly again (Figure 9f).

The mean annual SOC accumulation rates increased from 0.9 to 28.7 g $\mathrm{C\ m^{-2}yr^{-1}}$and from 0 to 57.1 g $\mathrm{C\ m^{-2}yr^{-1}}$ in the early-HTM (11-10 ka) for SP and SBP, respectively, with an area-weighted rate of 41.6 $\mathrm{C\ m^{-2}yr^{-1}}$ (Figure 11). The accumulation rate of the SP increased to 48.6 g $\mathrm{C\ m^{-2}yr^{-1}}$ while the rate of SBP slightly decreased to 56.7 g $\mathrm{C\ m^{-2}yr^{-1}}$ with an overall rate 54.7 $\mathrm{C\ m^{-2}yr^{-1}}$ in the late-HTM (10-9 ka) (Figure 11), followed by a drop to 22.7 and 13.1 g $\mathrm{C\ m^{-2}yr^{-1}}$ in the mid-Holocene (Figure 11). Late-Holocene rates ranged from 9.8 to -8.0 g $\mathrm{C\ m^{-2}yr^{-1}}$ for SP and SBP. The rates of SP and SBP reached 42.5 and 33.2 g $\mathrm{C\ m^{-2}yr^{-1}}$ respectively in the 20th century.

The change in total SOC stock corresponded well to the mean annual accumulation rates during the last 15,000 years (Figures 8, 11). A total of 37.4 Pg C was estimated to accumulate in Alaskan peatlands, with 23.9 Pg C in SP and 13.5 Pg C in SBP, from 15 ka to 2000 AD. The total peat C stock had an uncertainty range of 27-48 Pg C depending on model parameters (Table 4). The peatlands in the northern and southern coastal regions showed the highest SOC densities (>150 kg $\mathrm{C\ m^{-2}}$), while some central regions had the lowest (<20 kg $\mathrm{C\ m^{-2}}$) (Figure 12a). For newly formed peatlands in west central part and west coast, <100 kg $\mathrm{C\ m^{-2}}$ SOC was

Biogeosciences Discuss., doi:10.5194/bg-2016-284, 2016
Manuscript under review for journal Biogeosciences
Published: 14 July 2016

accumulated. The non-peatland SOC distribution was mainly decided by the vegetation types, with high densities (>15 kg C m^{-2}) in west and north coast where tundra dominated and low densities (<10 kg C m^{-2}) in central and east parts where boreal forests dominated (Figure 12b).

We used the observed mean C content of 46.8% in peat mass and bulk density of 166±76 kg m^{-3} in Alaska (Loisel et al., 2014) to estimate peat depth at each peat grid cell from the simulated peat SOC density (kg C m^{-2}). The spatial pattern of peat depth is identical to the SOC distribution, with most regions having peat depths of <2.5 m (Figure 12c). Based on the modern land area in each TEM gird cell and the inundation map, we estimated a weighted average depth of 1.9 m (ranging from 1.1 to 2.7 m, considering uncertainty in bulk density values) for Alaska peatlands. We also combined the SOC in both peatlands and non-peatlands results together to generate the total SOC distribution (Figure 12d). Soils at northern coast had the highest densities, many grids had SOC >40 kg C m^{-2}. Southwestern coast and eastern central Alaska also showed a high total SOC accumulation (>40 kg C m^{-2}). Central, eastern parts and west coast had the lowest SOC densities (<20 kg C m^{-2}).

3.4 Sensitivity Test

We found that NPP and decomposition rates changed simultaneously, but NPP had the dominant effect as the net SOC accumulation rate of Alaska increased and decreased under warmer and cooler conditions, respectively (Figures 13a, c, e). The net SOC accumulation rate increased as the condition became wetter and vice versa (Figures 13b, d, f). We also found an increase of SOC from 11.2 to 14.6 Pg C for upland mineral soils and 37.5 to 71 Pg C for peatlands after replacing the SP to SBP and upland forest systems with tundra. Meanwhile, under

Biogeosciences Discuss., doi:10.5194/bg-2016-284, 2016
Manuscript under review for journal Biogeosciences
Published: 14 July 2016

"warmer" and "wetter" conditions, the upland and peatland SOC increased by 13.8 Pg C and 35 Pg C, respectively.

4. Discussion

4.1 Effects of Climate on Ecosystem Carbon Accumulation

The simulated climate by ECBilt-CLIO model showed that among the six time periods, the coolest temperature appeared at 15-11 ka, followed by the late Holocene (5 ka-1900 AD). Those two periods were also generally dry (Figure 3f). The former represented colder and drier climate before the onset of the Holocene and the HTM (Barber and Finney, 2000; Edwards et al., 2001). The latter represented post-HTM neoglacial cooling, which caused permafrost aggradation across northern high latitudes (Oksanen et al., 2001; Zoltai, 1995).

The simulated NPP, vegetation C density and storage were highest during the HTM (Figures 5, 6). The highest C accumulation rates in both peatlands and non-peatlands occurred at the time (Figures 7-11). ECBilt-CLIO simulated an increase of temperature in the growing season (Figure 3c), also leading to a stronger seasonality of temperature during the HTM (Kaufman et al., 2004, 2016), caused by the maximum summer insolation (Berger and Loutre, 1991; Renssen et al., 2009). The highest mean annual and highest summer precipitations were also simulated during the 10-9 ka period. The highest vegetation C uptake and SOC accumulation rates coincided with the warmest summer and the wetter-than-before conditions, suggesting a strong link between those climate variables and C dynamics in Alaska. Enhanced climate seasonality characterized by warmer summer, enhanced summer precipitation and possibly earlier snow melt during the HTM increased NPP, as shown in our sensitivity test. Annual NPP increased by 40 and 20 g C m^{-2} yr^{-1} under the warmer and wetter scenarios,

Biogeosciences Discuss., doi:10.5194/bg-2016-284, 2016
Manuscript under review for journal Biogeosciences
Published: 14 July 2016

respectively (Figures 13a, b), indicating summer temperature and precipitation were the primary controls over NPP. Warmer condition could positively affect the SOC decomposition (Nobrega et al., 2007). Furthermore, hydrological effect can also be significant as higher precipitation could raise the water-table position, allowing less space for aerobic respiration. As shown in the sensitivity test, warmer and wetter could lead to an increase of decomposition up to 35 and 15 $\mathrm{g\,C\,m^{-2}\,yr^{-1}}$, respectively (Figures 13c, d). Such climatic effects on ecosystem productivity were consistent with modern studies (Tucker et al., 2001; Kimball et al., 2004; Linderholm, 2006). Our results did not show a decrease in total heterotrophic respiration throughout Alaska from the higher precipitation, presumably due to a much larger area of upland soils (1.3×10^6 $\mathrm{km^2}$) than peatland soils (0.26×10^6 $\mathrm{km^2}$), as higher precipitation would cause higher aerobic respiration in the unsaturated zone of upland soils. The relatively low vegetation NPP and C density, along with the low total vegetation and soil C stocks during 15-11 ka period and late-Holocene were consistent with the unfavorable cool and dry climate conditions (Figures 5, 6, 8, 11). Our previous simulations at four peatland sites in Alaska (Wang et al., 2016) suggested that temperature had the most significant effect on peat accumulation rate, followed by the seasonality of net solar radiation and temperature. Precipitation and the interactive effect from temperature and precipitation had some certain effects (p<0.05). The period from 15 to 11 ka experienced lower snowfall than the HTM. The combination of decreased snowfall and lower temperature could result in deeper frost depth due to the decreased insulative effects of the snowpack, and therefore shortening the period for active photosynthetic C uptake, leading to an overall low productivity (McGuire et al., 2000; Stieglitz et al., 2003). The positive effect of temperature on SOC accumulation as shown in this study, may help explain the coincidence between low SOC accumulation rates across the northern peatland domain and the cooler

Biogeosciences Discuss., doi:10.5194/bg-2016-284, 2016
Manuscript under review for journal Biogeosciences
Published: 14 July 2016

condition during the neoglacial period (Marcott et al., 2013; Vitt et al., 2000; Peteet et al., 1998; Yu et al. 2010). The stimulation of SOC accumulation from the warming and the rapid SOC accumulation rates during the 20th century in our study suggested a continue C sink will exist under the warmer and wetter climate conditions in the 21st century, as also concluded in Spahni et al. (2013).

The 20th century represented a temperature rise induced by global warming. It was still 1.1 °C lower than the late-HTM, suggesting the warmest climate during the HTM, which agreed with the previous study (Stafford et al., 2000). It was also lower than the mid-Holocene, which compared favorably with other estimates (Anderson and Brubaker, 1993; Kaufman et al., 2004). However, the annual precipitation during modern time estimated from other studies was higher than the HTM and mid-Holocene (Barber and Finney, 2000). The model output we used may overestimate the precipitation in the HTM, which could subsequently overestimate the water-table position and thus, the annual C accumulation rates. As studied, regional precipitation varies largely depending on the local topography (Stafford et al., 2000), thus the estimates with large-scale climate models have a large uncertainty. Great heterogeneity is produced from using large climatic controls (e.g., insolation and sea ice extent), which casts limits for accurately simulating the location- and topographic-specific climate data, especially precipitation (Whitlock and Bartlein, 1993; Mock and Bartlein, 1995).

4.2 Effects of Vegetation Distribution on Ecosystem Carbon Accumulation

Different vegetation distributions during various periods led to clear step changes, suggesting vegetation composition is likely to be the primary control on C dynamics. Similarly, SBP areas stored lower C than SP in overall at the spatial scale during each time period (Figure

9). Under cooler and drier climates, forested peatlands generally stopped accumulating SOC during the mid- and late-Holocene with some areas accompanied by a negative accumulation rate (Figures 9d,e), suggesting that such type of peatland could be more vulnerable to climate change due to its low C storage.

As key parameters controlling C dynamics in the model (e.g., maximum rate of photosynthesis, litter fall C) are ecosystem type specific, vegetation distribution change may have a dominant effect on simulated regional plant productivity and C storage. Our sensitivity test indicated that by replacing all vegetation types with forest systems, there was a total increase of 36.9 Pg in upland and peatland soils. There was also an increase of 48.8 Pg C under warmer and wetter conditions. These tests indicated that both climate and vegetation distribution have significant effects on C storage.

However, the high correlation between climate and ecosystem C dynamics as discussed above indicated that climate was probably the fundamental driver for vegetation composition changes over time. The vegetation changes as reconstructed from fossil pollen data during different time periods followed the general climate history during the last 15,000 years (He et al., 2014). Upland alpine and moist tundra stored the largest amounts of C due to their large areas among all vegetation types, as forests areas were limited before the HTM (Figure 6). On the basis of the observed relationship between the distributions of basal ages of peat samples and vegetation types (Table 2, Figure 2), alpine and moist tundra were favorable for peatlands initiation under a cooler climate. No forested peatlands formed before the HTM. Under the warm condition in the HTM, boreal evergreen needleleaf and deciduous broadleaf forests expanded (Figures 2b, c) as indicated by other studies (Bartlein et al., 2011; Edwards et al., 2005; Williams et al., 2001). Meanwhile, large areas were taken up by forested peatlands, characterized by the

Biogeosciences Discuss., doi:10.5194/bg-2016-284, 2016
Manuscript under review for journal Biogeosciences
Published: 14 July 2016

sharp increase of SOC storage in such ecosystems. The cooler temperature during the mid-Holocene limited the productivity of tree plants, leading to the retreat of trees. This is broadly consistent with other studies (Prentice et al., 1996; Edwards et al., 2000; Williams et al., 2001; Bigelow et al., 2003). Large proportion of forested peatlands thus changed back into *Sphagnum* spp. peatlands. The retreat of treeline on the Seward Peninsula in the cooler mid-Holocene likely reflects much shorter and cooler growing seasons, influenced by an expansion of sea ice in the Bering Sea (Crockford and Frederick, 2007) and the onset of the cooler Neoglacial climate. Forested peatlands ceased accumulating SOC in central Alaska with an overall low accumulation rates through the whole mid- to late-Holocene (Figures 8, 9, 11).

4.3 Comparison between Simulated Carbon Dynamics and Other Estimates

A large variation of "true" peat C accumulation rates was simulated on the Kenai Peninsula (Figure 4a), ranging from -4 (that is, peat C loss) to 50 $\mathrm{C\ m^{-2}\ yr^{-1}}$. We simulated an average of peat SOC "apparent" accumulation rate of 11.4 $\mathrm{g\ C\ m^{-2}\ yr^{-1}}$ from 15 to 5 ka (Figure 4b), which was slightly higher than the observed average rate from four sites (10.45 $\mathrm{g\ C\ m^{-2}\ yr^{-1}}$). The simulated rate during the HTM was 26.5 $\mathrm{g\ C\ m^{-2}\ yr^{-1}}$, up to five times higher than the rest of the Holocene (5.04 $\mathrm{g\ C\ m^{-2}\ yr^{-1}}$). The simulation results corresponded to the observations, in which an average rate of 20 $\mathrm{C\ m^{-2}\ yr^{-1}}$ from 11.5 to 8.6 ka was observed, four times higher than 5 $\mathrm{C\ m^{-2}\ yr^{-1}}$ over the rest of the Holocene.

We estimated an average peat SOC "apparent" accumulation rate of 13 $\mathrm{g\ C\ m^{-2} yr^{-1}}$ (2.3 $\mathrm{Tg\ C\ yr^{-1}}$ for the entire Alaska) from 15 ka to 2000 AD, lower than the value of 18.6 $\mathrm{g\ C\ m^{-2} yr^{-1}}$ as estimated from peat cores for northern peatlands (Yu et al., 2010), and slightly higher than the observed rate of 13.2 $\mathrm{g\ C\ m^{-2} yr^{-1}}$ from four peatlands in Alaska (Jones and Yu,

Biogeosciences Discuss., doi:10.5194/bg-2016-284, 2016
Manuscript under review for journal Biogeosciences
Published: 14 July 2016

2010). A simulated peak occurred during the HTM with the rate 29.1 g $\mathrm{C\ m^{-2}yr^{-1}}$ (5.1 Tg C $\mathrm{yr^{-1}}$), which was slightly higher than the observed 25 g $\mathrm{C\ m^{-2}yr^{-1}}$ for northern peatlands and ~20 g $\mathrm{C\ m^{-2}yr^{-1}}$ for Alaska (Yu et al., 2010). It was almost four times higher than the rate 6.9 g $\mathrm{C\ m^{-2}yr^{-1}}$ (1.4 Tg C $\mathrm{yr^{-1}}$) over the rest of the Holocene, which corresponded to the peat core-based observations of ~5 g $\mathrm{C\ m^{-2}yr^{-1}}$. The mid- and late Holocene showed much slower C accumulation at a rate approximately five folds lower than during the HTM. This corresponded to the observation of a six-fold decrease in the rate of new peatland formation after 8.6 ka (Jones and Yu 2010). The C accumulation rates increased abruptly to 39.2 g $\mathrm{C\ m^{-2}yr^{-1}}$during the last century, within the field-measured average apparent rate range of 20-50 g $\mathrm{C\ m^{-2}yr^{-1}}$ over the last 2000 years (Yu et al., 2010).

The SOC stock of northern peatlands has been estimated in many studies, ranging from 210 to 621 Pg (Oechel 1989; Gorham 1991; Armentano and Menges, 1986; Turunen et al., 2002; Yu et al., 2010; see Yu 2012 for a review). Assuming Alaskan peatlands were representative of northern peatlands and using the area of Alaskan peatlands (0.45×10^6 $\mathrm{km^2}$; Kivinen and Pakarinen, 1981) divided by the total area of northern peatlnads (~4×10^6 $\mathrm{km^2}$; Maltby and Immirzi 1993), we estimated a SOC stock of 23.6-69.9 Pg C for Alaskan peatlands. Our model estimated 27-48 Pg C had been accumulated from 15 ka to 2000 AD. The uncertainty may be resulted from peat basal age distributions and the peatland area, as we used modern inundation data to estimate an area of 0.26×10^6 $\mathrm{km^2}$. By incorporating the observed basal age distribution, we estimated that approximately 68% of Alaskan peatlands had formed by the end of the HTM, similar to the estimation from observed basal peat ages that 75% peatlands have formed by 8.6 ka (Jones and Yu 2010).

Biogeosciences Discuss., doi:10.5194/bg-2016-284, 2016
Manuscript under review for journal Biogeosciences
Published: 14 July 2016

The northern circumpolar soils were estimated to cover approximately 18.78×10^6 km^2 (Tarnocai et al., 2009). The non-peatland soil C stock was estimated to be in the range of 150-191 Pg C for boreal forests (Apps et al., 1993; Jobbagy and Jackson, 2000), and 60-144 Pg C for tundra (Apps et al., 1993; Gilmanov and Oechel, 1995; Oechel et al., 1993) in the 0-100 cm depth. Using the difference between Alaskan total land area (1.69×10^6 km^2) and peatland area (0.45×10^6 km^2), we estimated that the non-peatland area in Alaska was 1.24×10^6 km^2. Therefore, Alaska non-peatland area contained 17-27 Pg C by using the ratio of Alaskan non-peatland over northern non-peatland. In comparison, our estimate of 9-15 Pg C within 1-meter depth suggested that our model might have underestimated the C stock for non-peatland soils. Meanwhile, our estimated 2.5-3.7 Pg C stored in the Alaskan vegetation was lower than the previous estimate of 5 Pg (Balshi et al., 2007; McGuire et al., 2009). The underestimation could be resulted from the uncertainties in both peatland area fraction within each grid and the model parameterization.

The simulated modern SOC distribution (Figure 12c) was largely consistent with the study of Hugelius et al. (2014) (see Figure 3 in the paper). The model captured the high peat SOC density areas on northern and southwestern coasts of Alaska, where observational data showed some locations with SOC >75 kg C m^{-2}. This corresponded to our model simulation that many grids had the SOC >75 kg C m^{-2} in those areas. The observed overall average SOC density of >40 kg C m^{-2} was also consistent with our simulation. Eastern part and west coast had the lowest SOC densities, corresponding to the model result that most grids in those areas had SOC values between 20 and 40 kg C m^{-2}. Our estimated average peat depth of 1.9 m ranging from 1.1 to 2.7 m from simulated peat SOC density was similar to the observed mean depth of 2.29 m for Alaskan peatlands (Gorham et al., 1991, 2012). Our estimates (Figure 12d) showed a

Biogeosciences Discuss., doi:10.5194/bg-2016-284, 2016
Manuscript under review for journal Biogeosciences
Published: 14 July 2016

high correlation with the 64 observed peat samples (Figure 14) ($R^2 = 0.45$). The large intercept of the regression line (101 cm) suggested that the model may not perform well in estimating the grids with low peat depths (<50 cm).

5. Conclusions

We used a biogeochemistry model for both peatland and non-peatland ecosystems to quantify the C stock and its changes over time in terrestrial ecosystems of Alaska during the last 15,000 years. The simulated peat SOC accumulation rates were compared with peat-core data from four peatlands on the Kenai Peninsula in southern Alaska. The model well estimated the peat SOC accumulation rates trajectory throughout the Holocene, indicating the model's suitability for simulating peat C dynamics. Our regional simulation showed that 36-63 Pg C had been accumulated in Alaskan land ecosystems since 15,000 years ago, including 27-48 Pg C in peatlands and 9-15 Pg C in non-peatlands (within 1 m depth). We also estimated that 2.5-3.7 Pg C was stored in contemporary Alaskan vegetation, with 0.3-0.6 Pg C in peatlands and 2.2-3.1 Pg C in non-peatlands. The estimated average rate of peat C accumulation was 2.3 Tg C yr^{-1} with a peak (5.1 Pg C yr^{-1}) in the Holocene Thermal Maximum (HTM), four folds higher than the rate of 1.4 Pg C yr^{-1} over the rest of the Holocene. The 20$^{\text{th}}$ century represented another high SOC accumulation period after the much lowered accumulation rate in the late Holocene. We estimated an average depth of 1.9 m of peat in Alaskan peatlands, similar to the observed mean depth. We found that the changes of vegetation distribution due to the climatic change were the key factors to the spatial variations of SOC accumulation in different time periods. The warming in the HTM characterized by the increased summer temperature and increased seasonality of solar radiation, along with the higher precipitation might have played an important role in

Biogeosciences Discuss., doi:10.5194/bg-2016-284, 2016
Manuscript under review for journal Biogeosciences
Published: 14 July 2016

causing the high C accumulation rates. Under warming climate conditions, Alaskan peatlands may continue acting as C sink in the future.

6. Acknowledgment. We acknowledge the funding support from a NSF project IIS-1027955 and a DOE project DE-SC0008092. We also acknowledge the SPRUCE project to allow us use its data. Data presented in this paper are publicly accessible: ECBilt-CLIO Paleosimulation (http://apdrc.soest.hawaii.edu/datadoc/sim2bl.php), CRU2.0 (http://www.cru.uea.ac.uk/data). Model parameter data and model evaluation process are in Wang et al. (2016). Other simulation data including model codes are available upon request from the corresponding author (qzhuang@purdue.edu).

7. References

Anderson, P. M., & Brubaker, L. B. (1993). Holocene vegetation and climate histories of Alaska. *Global climates since the last glacial maximum*, 385-400.

Apps, M. J., Kurz, W. A., Luxmoore, R. J., Nilsson, L. O., Sedjo, R. A., Schmidt, R., ... & Vinson, T. S. (1993). Boreal forests and tundra. *Water, Air, and Soil Pollution*, *70*(1-4), 39-53.

Armentano, T. V., & Menges, E. S. (1986). Patterns of change in the carbon balance of organic soil-wetlands of the temperate zone. *The Journal of Ecology*, 755-774.

Assessment, A. C. I. (2005). Forests, land management and agriculture.*Arctic Climate Impact Assessment*, 781-862.

Balshi, M. S., McGuire, A. D., Zhuang, Q., Melillo, J., Kicklighter, D. W., Kasischke, E., ... & Burnside, T. J. (2007). The role of historical fire disturbance in the carbon dynamics of the pan-boreal region: A process-based analysis. *Journal of Geophysical Research: Biogeosciences*, *112*(G2).

Barber, V. A., & Finney, B. P. (2000). Late Quaternary paleoclimatic reconstructions for interior Alaska based on paleolake-level data and hydrologic models. *Journal of Paleolimnology*, *24*(1), 29-41.

Bartlein, P. J., Harrison, S. P., Brewer, S., Connor, S., Davis, B. A. S., Gajewski, K., ... & Prentice, I. C. (2011). Pollen-based continental climate reconstructions at 6 and 21 ka: a global synthesis. *Climate Dynamics*, *37*(3-4), 775-802.

Belyea, L. R. (2009). Nonlinear dynamics of peatlands and potential feedbacks on the climate system. *Carbon cycling in northern peatlands*, 5-18.

Biogeosciences Discuss., doi:10.5194/bg-2016-284, 2016
Manuscript under review for journal Biogeosciences
Published: 14 July 2016

Berger, A., & Loutre, M. F. (1991). Insolation values for the climate of the last 10 million years. *Quaternary Science Reviews*, *10*(4), 297-317.

Bigelow, N. H., Brubaker, L. B., Edwards, M. E., Harrison, S. P., Prentice, I. C., Anderson, P. M., ... & Kaplan, J. O. (2003). Climate change and Arctic ecosystems: 1. Vegetation changes north of 55 N between the last glacial maximum, mid-Holocene, and present. *Journal of Geophysical Research: Atmospheres*, *108*(D19).

Bridgham, S. D., Megonigal, J. P., Keller, J. K., Bliss, N. B., & Trettin, C. (2006). The carbon balance of North American wetlands. *Wetlands*, *26*(4), 889-916.

Carter, A. J., & Scholes, R. J. (2000). SoilData v2. 0: generating a global database of soil properties. *Environmentek CSIR, Pretoria, South Africa*.

Change, I. C. (2013). The Physical Science Basis: Working Group I Contribution to the Fifth Assessment Report of the Intergovernmental Panel on Climate Change. *New York: Cambridge University Press*, *1*, 535-1.

Change, I. C. (2014). Mitigation of Climate Change. Contribution of Working Group III to the Fifth Assessment Report of the Intergovernmental Panel on Climate Change. *Cambridge University Press, Cambridge, UK and New York, NY*.

Chivers, M. R., Turetsky, M. R., Waddington, J. M., Harden, J. W., & McGuire, A. D. (2009). Effects of experimental water table and temperature manipulations on ecosystem CO2 fluxes in an Alaskan rich fen.*Ecosystems*, *12*(8), 1329-1342.

Churchill, A. (2011). The response of plant community structure and productivity to changes in hydrology in Alaskan boreal peatlands. *Master Thesis*, University of Alaska, Fairbanks, AK, USA. 119 pp.

Conrad, R. (1999). Contribution of hydrogen to methane production and control of hydrogen concentrations in methanogenic soils and sediments.*FEMS Microbiology Ecology*, *28*(3), 193-202.

Crockford, S. J., & Frederick, S. G. (2007). Sea ice expansion in the Bering Sea during the Neoglacial: Evidence from archaeozoology. *The Holocene*,*17*(6), 699-706.

Davidson, E. A., Trumbore, S. E., & Amundson, R. (2000). Biogeochemistry: soil warming and organic carbon content. *Nature*, *408*(6814), 789-790.

Davidson, E. A., & Janssens, I. A. (2006). Temperature sensitivity of soil carbon decomposition and feedbacks to climate change. *Nature*, *440*(7081), 165-173.

Edwards, M. E., Anderson, P. M., Brubaker, L. B., Ager, T. A., Andreev, A. A., Bigelow, N. H., ... & Jolly, D. (2000). Pollen-based biomes for Beringia 18,000, 6000 and 0 14C yr bp. *Journal of Biogeography*, *27*(3), 521-554.

Edwards, M. E., Mock, C. J., Finney, B. P., Barber, V. A., & Bartlein, P. J. (2001). Potential analogues for paleoclimatic variations in eastern interior Alaska during the past 14,000 yr: atmospheric-circulation controls of regional temperature and moisture responses. *Quaternary Science Reviews*, *20*(1), 189-202.

Edwards, M. E., Brubaker, L. B., Lozhkin, A. V., & Anderson, P. M. (2005). Structurally novel biomes: a response to past warming in Beringia. *Ecology*,*86*(7), 1696-1703.

Euskirchen, E. S., McGuire, A. D., & Chapin, F. S. (2007). Energy feedbacks of northern high-latitude ecosystems to the climate system due to reduced snow cover during 20th century warming. *Global Change Biology*,*13*(11), 2425-2438.

Frolking, S., Roulet, N. T., Tuittila, E., Bubier, J. L., Quillet, A., Talbot, J., & Richard, P. J. H. (2010). A new model of Holocene peatland net primary production, decomposition, water balance, and peat accumulation. *Earth System Dynamics*, *1*(1), 1-21.

Frolking, S., Talbot, J., Jones, M. C., Treat, C. C., Kauffman, J. B., Tuittila, E. S., & Roulet, N. (2011). Peatlands in the Earth's 21st century climate system. *Environmental Reviews*, *19*(NA), 371-396.

Gilmanov, T. G., & Oechel, W. C. (1995). New estimates of organic matter reserves and net primary productivity of the North American tundra ecosystems. *Journal of Biogeography*, 723-741.

Gorham, E. V. I. L. L. E. (1990). Biotic impoverishment in northern peatlands. *The earth in transition: patterns and processes of biotic impoverishment. Cambridge University Press, Cambridge, UK*, 65-98.

Gorham, E. (1991). Northern peatlands: role in the carbon cycle and probable responses to climatic warming. *Ecological applications*, *1*(2), 182-195.

Gorham, E., Lehman, C., Dyke, A., Clymo, D., & Janssens, J. (2012). Long-term carbon sequestration in North American peatlands. *Quaternary Science Reviews*, *58*, 77-82.

He, Y., Jones, M. C., Zhuang, Q., Bochicchio, C., Felzer, B. S., Mason, E., & Yu, Z. (2014). Evaluating CO 2 and CH 4 dynamics of Alaskan ecosystems during the Holocene Thermal Maximum. *Quaternary Science Reviews*, *86*, 63-77.

Hinzman, L. D., Viereck, L. A., Adams, P. C., Romanovsky, V. E., & Yoshikawa, K. (2006). Climate and permafrost dynamics of the Alaskan boreal forest. *Alaska's Changing Boreal Forest*, 39-61.

Hobbie, S. E. (2000). Interactions between litter lignin and nitrogenitter lignin and soil nitrogen availability during leaf litter decomposition in a Hawaiian montane forest. *Ecosystems*, *3*(5), 484-494.

Hugelius, G., Strauss, J., Zubrzycki, S., Harden, J. W., Schuur, E., Ping, C. L., ... & O'Donnell, J. A. (2014). Estimated stocks of circumpolar permafrost carbon with quantified uncertainty ranges and identified data gaps.*Biogeosciences*, *11*(23), 6573-6593.

Huybers, P. (2006). Early Pleistocene glacial cycles and the integrated summer insolation forcing. *Science*, *313*(5786), 508-511.

Jobbágy, E. G., & Jackson, R. B. (2000). The vertical distribution of soil organic carbon and its relation to climate and vegetation. *Ecological applications*, *10*(2), 423-436.

Jones, M. C., & Yu, Z. (2010). Rapid deglacial and early Holocene expansion of peatlands in Alaska. *Proceedings of the National Academy of Sciences*,*107*(16), 7347-7352.

Jones, P. D., & Moberg, A. (2003). Hemispheric and large-scale surface air temperature variations: An extensive revision and an update to 2001. *Journal of Climate*, *16*(2), 206-223.

Biogeosciences Discuss., doi:10.5194/bg-2016-284, 2016
Manuscript under review for journal Biogeosciences
Published: 14 July 2016

Kane, E. S., Turetsky, M. R., Harden, J. W., McGuire, A. D., & Waddington, J. M. (2010). Seasonal ice and hydrologic controls on dissolved organic carbon and nitrogen concentrations in a boreal-rich fen. *Journal of Geophysical Research: Biogeosciences*, *115*(G4).

Kaufman, D. S., Ager, T. A., Anderson, N. J., Anderson, P. M., Andrews, J. T., Bartlein, P. J., ... & Dyke, A. S. (2004). Holocene thermal maximum in the western Arctic (0–180 W). *Quaternary Science Reviews*, *23*(5), 529-560.

Kaufman, D.S., Axford, Y.L., Henerson, A., McKay, N.P., Oswald, W.W., Saenger, C., Anderson, R.S., Bailey, H.L., Clegg, B., Gajewski, K., Hu, F.S., Jones, M.C., Massa, C., Routson, C.C., Werner, A., Wooller, M.J., Yu, Z., 2016. Holocene climate changes in eastern Beringia (NW North America) e a systemic review of multi-proxy evidence. *Quaternary Science Reviews,* this volume. http://dx.doi.org/10.1016/ j.quascirev.2015.10.021.

Keller, J. K., & Bridgham, S. D. (2007). Pathways of anaerobic carbon cycling across an ombrotrophic–minerotrophic peatland gradient.

Keller, J. K., & Takagi, K. K. (2013). Solid-phase organic matter reduction regulates anaerobic decomposition in bog soil. *Ecosphere*, *4*(5), 1-12.

Kimball, J. S., McDonald, K. C., Running, S. W., & Frolking, S. E. (2004). Satellite radar remote sensing of seasonal growing seasons for boreal and subalpine evergreen forests. *Remote Sensing of Environment*, *90*(2), 243-258.

Kivinen, E., and P. Pakarinen. (1981). Geographical distribution of peat resources and major peatland complex types in the world. Annales Academiae Scientarum Fennicae, Series A, Number 132.

Kleinen, T., Brovkin, V., von Bloh, W., Archer, D., & Munhoven, G. (2010). Holocene carbon cycle dynamics. *Geophysical Research Letters*, *37*(2).

Kuhry, P., & Vitt, D. H. (1996). Fossil carbon/nitrogen ratios as a measure of peat decomposition. *Ecology*, *77*(1), 271-275.

Linderholm, H. W. (2006). Growing season changes in the last century.*Agricultural and Forest Meteorology*, *137*(1), 1-14.

Loisel, J., Gallego-Sala, A. V., & Yu, Z. (2012). Global-scale pattern of peatland Sphagnum growth driven by photosynthetically active radiation and growing season length. *Biogeosciences*, *9*(7), 2737-2746.

Loisel, J., Yu, Z., Beilman, D. W., Camill, P., Alm, J., Amesbury, M. J., ... & Belyea, L. R. (2014). A database and synthesis of northern peatland soil properties and Holocene carbon and nitrogen accumulation. *the Holocene*, 0959683614538073.

Maltby, E., & Immirzi, P. (1993). Carbon dynamics in peatlands and other wetland soils regional and global perspectives. *Chemosphere*, *27*(6), 999-1023.

Manabe, S., & Wetherald, R. T. (1980). On the distribution of climate change resulting from an increase in CO2 content of the atmosphere. *Journal of the Atmospheric Sciences*, *37*(1), 99-118.

Manabe, S., & Wetherald, R. T. (1986). Reduction in summer soil wetness induced by an increase in atmospheric carbon dioxide. *Science*, *232*(4750), 626-628.

Marcott, S. A., Shakun, J. D., Clark, P. U., & Mix, A. C. (2013). A reconstruction of regional and global temperature for the past 11,300 years.*science*, *339*(6124), 1198-1201.

Matthews, E., & Fung, I. (1987). Methane emission from natural wetlands: Global distribution, area, and environmental characteristics of sources.*Global biogeochemical cycles*, *1*(1), 61-86.

McGuire, A. D., Melillo, J. M., Kicklighter, D. W., & Joyce, L. A. (1995). Equilibrium responses of soil carbon to climate change: empirical and process-based estimates. *Journal of Biogeography*, 785-796.

McGuire, A. D., & Hobbie, J. E. (1997). Global climate change and the equilibrium responses of carbon storage in arctic and subarctic regions. In*Modeling the Arctic system: A workshop report on the state of modeling in the Arctic System Science program* (pp. 53-54).

McGuire, A. D., Melillo, J. M., Randerson, J. T., Parton, W. J., Heimann, M., Meier, R. A., ... & Sauf, W. (2000). Modeling the effects of snowpack on heterotrophic respiration across northern temperate and high latitude regions: Comparison with measurements of atmospheric carbon dioxide in high latitudes. *Biogeochemistry*, *48*(1), 91-114.

McGuire, A. D., Anderson, L. G., Christensen, T. R., Dallimore, S., Guo, L., Hayes, D. J., ... & Roulet, N. (2009). Sensitivity of the carbon cycle in the Arctic to climate change. *Ecological Monographs*, *79*(4), 523-555.

Melillo, J. M., Kicklighter, D. W., McGuire, A. D., Peterjohn, W. T., & Newkirk, K. (1995, July). Global change and its effects on soil organic carbon stocks. In *Dahlem Conference Proceedings, John Wiley and Sons, New York, John Wiley & Sons, Ltd., Chichster* (pp. 175-189).

Mock, C. J., & Bartlein, P. J. (1995). Spatial variability of late-Quaternary paleoclimates in the western United States. *Quaternary Research*, *44*(3), 425-433.

Moore, T. R., Bubier, J. L., Frolking, S. E., Lafleur, P. M., & Roulet, N. T. (2002). Plant biomass and production and CO2 exchange in an ombrotrophic bog. *Journal of Ecology*, *90*(1), 25-36.

Nobrega, S., & Grogan, P. (2007). Deeper snow enhances winter respiration from both plant-associated and bulk soil carbon pools in birch hummock tundra. *Ecosystems*, *10*(3), 419-431.

Oechel, W. C. (1989). Nutrient and water flux in a small arctic watershed: an overview. *Holarctic Ecology*, 229-237.

Oechel, W. C., Hastings, S. J., Vourlrtis, G., Jenkins, M., Riechers, G., & Grulke, N. (1993). Recent change of Arctic tundra ecosystems from a net carbon dioxide sink to a source. *Nature*, *361*(6412), 520-523.

Oksanen, P. O., Kuhry, P., & Alekseeva, R. N. (2001). Holocene development of the Rogovaya river peat plateau, European Russian Arctic.*The Holocene*, *11*(1), 25-40.

Peteet, D., Andreev, A., Bardeen, W., & Mistretta, F. (1998). Long-term Arctic peatland dynamics, vegetation and climate history of the Pur-Taz region, western Siberia. *Boreas*, *27*(2), 115-126.

Prentice, C., Guiot, J., Huntley, B., Jolly, D., & Cheddadi, R. (1996). Reconstructing biomes from palaeoecological data: a general method and its application to European pollen data at 0 and 6 ka. *Climate Dynamics*, *12*(3), 185-194.

Prentice, I. C. (2008). Terrestrial nitrogen cycle simulation with a dynamic global vegetation model. *Global Change Biology*, *14*(8), 1745-1764.

Biogeosciences Discuss., doi:10.5194/bg-2016-284, 2016
Manuscript under review for journal Biogeosciences
Published: 14 July 2016

Raich, J. W., Rastetter, E. B., Melillo, J. M., Kicklighter, D. W., Steudler, P. A., Peterson, B. J., ... & Vorosmarty, C. J. (1991). Potential net primary productivity in South America: application of a global model. *Ecological Applications*, *1*(4), 399-429.

Renssen, H., Seppä, H., Heiri, O., Roche, D. M., Goosse, H., & Fichefet, T. (2009). The spatial and temporal complexity of the Holocene thermal maximum. *Nature Geoscience*, *2*(6), 411-414.

Roulet, N. T., Lafleur, P. M., Richard, P. J., Moore, T. R., Humphreys, E. R., & Bubier, J. I. L. L. (2007). Contemporary carbon balance and late Holocene carbon accumulation in a northern peatland. *Global Change Biology*, *13*(2), 397-411.

Schuur, E. A., Bockheim, J., Canadell, J. G., Euskirchen, E., Field, C. B., Goryachkin, S. V., ... & Mazhitova, G. (2008). Vulnerability of permafrost carbon to climate change: implications for the global carbon cycle.*BioScience*, *58*(8), 701-714.

Sitch, S., Smith, B., Prentice, I. C., Arneth, A., Bondeau, A., Cramer, W., ... & Thonicke, K. (2003). Evaluation of ecosystem dynamics, plant geography and terrestrial carbon cycling in the LPJ dynamic global vegetation model.*Global Change Biology*, *9*(2), 161-185.

Spahni, R., Joos, F., Stocker, B. D., Steinacher, M., & Yu, Z. C. (2013). Transient simulations of the carbon and nitrogen dynamics in northern peatlands: from the Last Glacial Maximum to the 21st century. *Climate of the Past*, *9*(3), 1287-1308.

Stafford, J. M., Wendler, G., & Curtis, J. (2000). Temperature and precipitation of Alaska: 50 year trend analysis. *Theoretical and Applied Climatology*, *67*(1-2), 33-44.

Stieglitz, M., Déry, S. J., Romanovsky, V. E., & Osterkamp, T. E. (2003). The role of snow cover in the warming of arctic permafrost. *Geophysical Research Letters*, *30*(13).

Stocker, B. D., Strassmann, K., & Joos, F. (2011). Sensitivity of Holocene atmospheric CO 2 and the modern carbon budget to early human land use: analyses with a process-based model. *Biogeosciences*, *8*(1), 69-88.

Stocker, B. D., Spahni, R., & Joos, F. (2014). DYPTOP: a cost-efficient TOPMODEL implementation to simulate sub-grid spatio-temporal dynamics of global wetlands and peatlands. *Geoscientific Model Development*, *7*(6), 3089-3110.

Tang, J., & Zhuang, Q. (2008). Equifinality in parameterization of process-based biogeochemistry models: A significant uncertainty source to the estimation of regional carbon dynamics. *Journal of Geophysical Research: Biogeosciences*, *113*(G4).

Tang, J., & Zhuang, Q. (2009). A global sensitivity analysis and Bayesian inference framework for improving the parameter estimation and prediction of a process-based Terrestrial Ecosystem Model. *Journal of Geophysical Research: Atmospheres*, *114*(D15).

Tang, J., Zhuang, Q., Shannon, R. D., & White, J. R. (2010). Quantifying wetland methane emissions with process-based models of different complexities. *Biogeosciences*, *7*(11), 3817-3837.

Tarnocai, C., Canadell, J. G., Schuur, E. A. G., Kuhry, P., Mazhitova, G., & Zimov, S. (2009). Soil organic carbon pools in the northern circumpolar permafrost region. *Global biogeochemical cycles*, *23*(2).

Biogeosciences Discuss., doi:10.5194/bg-2016-284, 2016
Manuscript under review for journal Biogeosciences
Published: 14 July 2016

Timmermann, A., Timm, O., Stott, L., & Menviel, L. (2009). The roles of CO2 and orbital forcing in driving southern hemispheric temperature variations during the last 21 000 Yr*. *Journal of Climate*, *22*(7), 1626-1640.

Tucker, C. J., Slayback, D. A., Pinzon, J. E., Los, S. O., Myneni, R. B., & Taylor, M. G. (2001). Higher northern latitude normalized difference vegetation index and growing season trends from 1982 to 1999. *International journal of biometeorology*, *45*(4), 184-190.

Turetsky, M. R., Treat, C. C., Waldrop, M. P., Waddington, J. M., Harden, J. W., & McGuire, A. D. (2008). Short-term response of methane fluxes and methanogen activity to water table and soil warming manipulations in an Alaskan peatland. *Journal of Geophysical Research: Biogeosciences*,*113*(G3).

Turunen, J., Tomppo, E., Tolonen, K., & Reinikainen, A. (2002). Estimating carbon accumulation rates of undrained mires in Finland–application to boreal and subarctic regions. *The Holocene*, *12*(1), 69-80.

Vitt, D. H., Halsey, L. A., Bauer, I. E., & Campbell, C. (2000). Spatial and temporal trends in carbon storage of peatlands of continental western Canada through the Holocene. *Canadian Journal of Earth Sciences*, *37*(5), 683-693.

Wang, S., Zhuang, Q., Yu, Z., Bridgham, S., & Keller, J. (2016). Quantifying peat carbon accumulation in Alaska using a process-based biogeochemistry model. *Journal of Geophysical Research: Biogeosciences* (Under revision).

Whitlock, C., & Bartlein, P. J. (1993). Spatial variations of Holocene climatic change in the Yellowstone region. *Quaternary Research*, *39*(2), 231-238.

Williams, J. W., Webb, T., Richard, P. H., & Newby, P. (2000). Late Quaternary biomes of Canada and the eastern United States. *Journal of Biogeography*, *27*(3), 585-607.

Yu, Z., Beilman, D. W., & Jones, M. C. (2009). Sensitivity of northern peatland carbon dynamics to Holocene climate change. *Carbon cycling in northern peatlands*, 55-69.

Yu, Z., Loisel, J., Brosseau, D. P., Beilman, D. W., & Hunt, S. J. (2010). Global peatland dynamics since the Last Glacial Maximum. *Geophysical Research Letters*, *37*(13).

Yu, Z. C. (2012). Northern peatland carbon stocks and dynamics: a review.*Biogeosciences*, *9*(10), 4071-4085.

Zhuang, Q., Romanovsky, V. E., & McGuire, A. D. (2001). Incorporation of a permafrost model into a large-scale ecosystem model: Evaluation of temporal and spatial scaling issues in simulating soil thermal dynamics.*Journal of Geophysical Research: Atmospheres*, *106*(D24), 33649-33670.

Zhuang, Q., McGuire, A. D., O'neill, K. P., Harden, J. W., Romanovsky, V. E., & Yarie, J. (2002). Modeling soil thermal and carbon dynamics of a fire chronosequence in interior Alaska. *Journal of Geophysical Research: Atmospheres*, *107*(D1).

Zhuang, Q., McGuire, A. D., Melillo, J. M., Clein, J. S., Dargaville, R. J., Kicklighter, D. W., ... & Hobbie, J. E. (2003). Carbon cycling in extratropical terrestrial ecosystems of the Northern Hemisphere during the 20th century: a modeling analysis of the influences of soil thermal dynamics. *Tellus B*, *55*(3), 751-776.

Zhuang, Q., Melillo, J. M., Kicklighter, D. W., Prinn, R. G., McGuire, A. D., Steudler, P. A., ... & Hu, S. (2004). Methane fluxes between terrestrial ecosystems and the atmosphere at northern high latitudes during the past century: A retrospective analysis with a process-based biogeochemistry model. *Global Biogeochemical Cycles*, *18*(3).

Zhuang, Q., Zhu, X., He, Y., Prigent, C., Melillo, J. M., McGuire, A. D., ... & Kicklighter, D. W. (2015). Influence of changes in wetland inundation extent on net fluxes of carbon dioxide and methane in northern high latitudes from 1993 to 2004. *Environmental Research Letters*, *10*(9), 095009.

Zimov, S. A., Schuur, E. A., & Chapin III, F. S. (2006). Permafrost and the global carbon budget. *Science(Washington)*, *312*(5780), 1612-1613.

Zoltai, S. C. (1995). Permafrost distribution in peatlands of west-central Canada during the Holocene warm period 6000 years BP. *Géographie physique et Quaternaire*, *49*(1), 45-54.

Biogeosciences Discuss., doi:10.5194/bg-2016-284, 2016
Manuscript under review for journal Biogeosciences
Published: 14 July 2016

Biogeosciences Discussions
Open Access
EGU

Table 1. Assignment of biomized fossil pollen data to the vegetation types in TEM (He et al., 2014).

TEM upland vegetation	TEM peatland vegetation	BIOMISE code
Alpine tundra		CUSH DRYT PROS
Moist tundra	*Sphagnum* spp. open fen	DWAR SHRU
Boreal evergreen needleleaf and mixed forest	*Sphagnum*-black spruce bog	TAIG COCO CLMX COMX
Boreal deciduous broadleaf forest		CLDE

Table 2. Relations between peatland basal age and vegetation distribution

Peatland basal age	Vegetation types	Location
15-11 ka	alpine tundra	south, northwestern, and southeastern coast
11-10 ka	moist tundra boreal evergreen needleleaf forest boreal deciduous broadleaf forest	south, north, and southeastern coast east central part
10-9 ka	moist tundra boreal evergreen needleleaf forest boreal deciduous broadleaf forest	south and north coast central part
9-5 ka	moist tundra boreal evergreen needleleaf forest	central part
5 ka-1900 AD	moist tundra boreal evergreen needleleaf forest	west coast

Biogeosciences Discuss., doi:10.5194/bg-2016-284, 2016
Manuscript under review for journal Biogeosciences
Published: 14 July 2016

Table 3. Description of sites and variables used for parameterizing the core carbon and nitrogen module (CNDM).

Site[a]	Vegetation	Observed variables for CNDM parameterization	References
APEXCON	Moderate rich open fen with sedges (*Carex* sp.), spiked rushes (*Eleocharis* sp.), *Sphagnum* spp., and brown mosses (e.g., *Drepanocladus aduncus*)	Mean annual aboveground NPP in 2009; Mean annual belowground NPP in 2009; Aboveground biomass in 2009	Chivers et al. (2009) Turetsky et al. (2008) Kane et al. (2010) Churchill et al. (2011)
APEXPER	Peat plateau bog with black spruce (*Picea mariana*), *Sphagnum* spp., and feather mosses		

[a]The Alaskan Peatland Experiment (APEX) site is adjacent to the Bonanza Creek Experimental Forest (BCEF) site, approximately 35 km southwest of Fairbanks, AK. The area is classified as continental boreal climate with a mean annual temperature of -2.9℃ and annual precipitation of 269 mm, of which 30% is snow (Hinzman et al., 2006).

Table 4. Carbon pools and fluxes used for calibration of CMDM

Annual Carbon Fluxes or Pools[a]	*Sphagnum* Open Fen		*Sphagnum*-Black Spruce Bog		References
	Observation	Simulation	Observation	Simulation	
NPP	445±260	410	433±107	390	Turetsky et al. (2008), Churchill (2011) Moore et al. (2002) Zhuang et al. (2002) Tarnocai et al. (2009) Kuhry and Vitt (1996)
Aboveground Vegetation Carbon	149-287		423		
Belowground Vegetation Carbon	564		658-1128		
Total Vegetation Carbon Density	713-851	800	732-1551	1300	
Litter Fall Carbon Flux	300	333	300	290	
Methane Emission Flux	19.5	19.2	9.7	12.8	

[a] Units for annual net primary production (NPP) and litter fall carbon are $\mathrm{g\ C\ m^{-2}\ yr^{-1}}$. Units for vegetation carbon density are $\mathrm{g\ C\ m^{-2}}$. Units for Methane emissions are $\mathrm{g\ C-CH_4\ m^{-2}\ yr^{-1}}$. The simulated total annual methane fluxes were compared with the observations at APEXCON in 2005 and SPRUCE in 2012. A ratio of 0.47 was used to convert vegetation biomass to carbon (Raich 1991).

Biogeosciences Discuss., doi:10.5194/bg-2016-284, 2016
Manuscript under review for journal Biogeosciences
Published: 14 July 2016

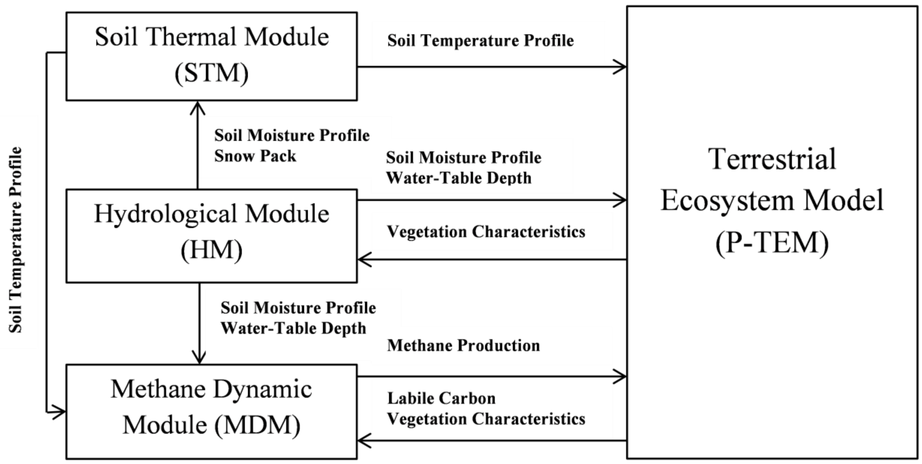

Figure 1. P-TEM (Peatland-Terrestrial Ecosystem Model) modeling framework, including a soil thermal module (STM), a hydrologic module (HM), a carbon/ nitrogen dynamic model (CNDM), and a methane dynamics module (MDM) (Wang et al., 2016).

Biogeosciences Discuss., doi:10.5194/bg-2016-284, 2016
Manuscript under review for journal Biogeosciences
Published: 14 July 2016

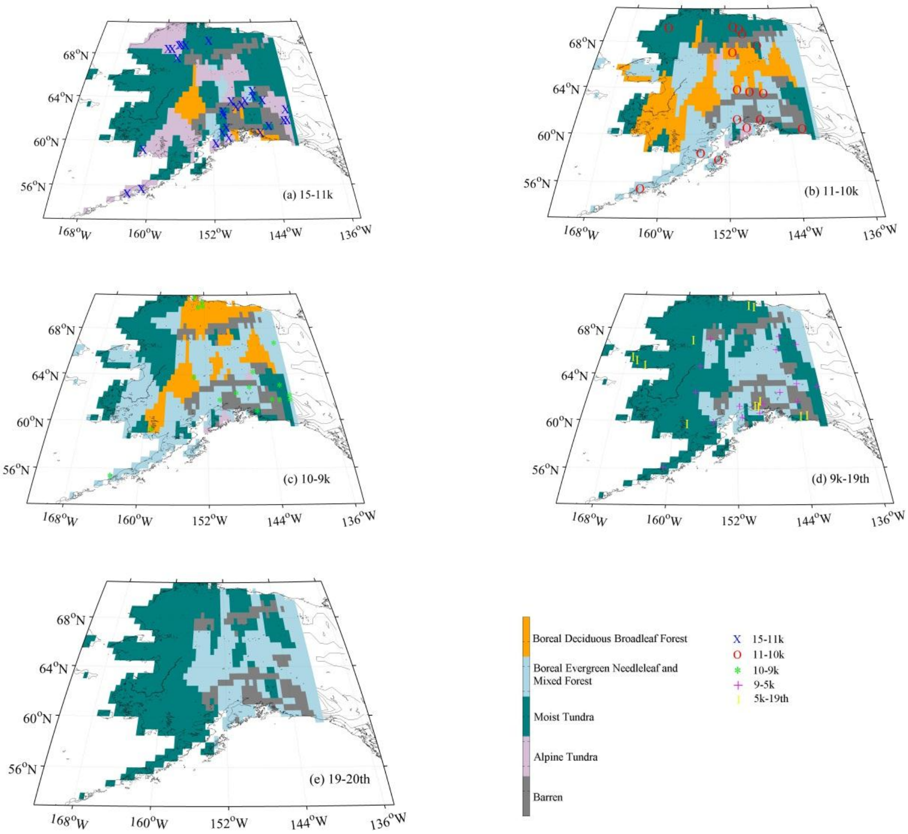

Figure 2. Alaskan vegetation distribution maps reconstructed from fossil pollen data during (a) 15-11 ka, (b) 11-10 ka, (c) 10-9 ka, (d) 9 ka -1900 AD, and (e) 1900-2000 AD (He et al., 2014). Symbols represent the basal age of peat samples (n = 102) in Gorham et al. (2012). Barren refers to mountain range and large body areas which could not be interpolated.

Biogeosciences Discuss., doi:10.5194/bg-2016-284, 2016
Manuscript under review for journal Biogeosciences
Published: 14 July 2016

Biogeosciences
Discussions
Open Access

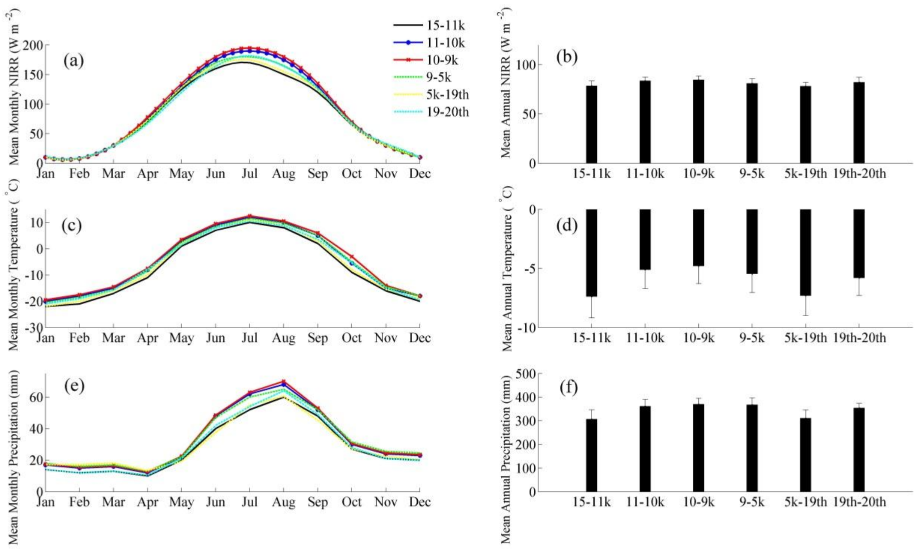

Figure 3. Simulated Paleo-climate and other input data from 15 ka to 2000 AD, including (a) mean monthly and (b) mean annual net incoming solar radiation (NIRR, W m^{-2}), (c) mean monthly and (d) mean annual air temperature (℃), (e) mean monthly and (f) mean annual precipitation (mm) (Timm and Timmermann, 2007; He et al., 2014).

Biogeosciences Discuss., doi:10.5194/bg-2016-284, 2016
Manuscript under review for journal Biogeosciences
Published: 14 July 2016

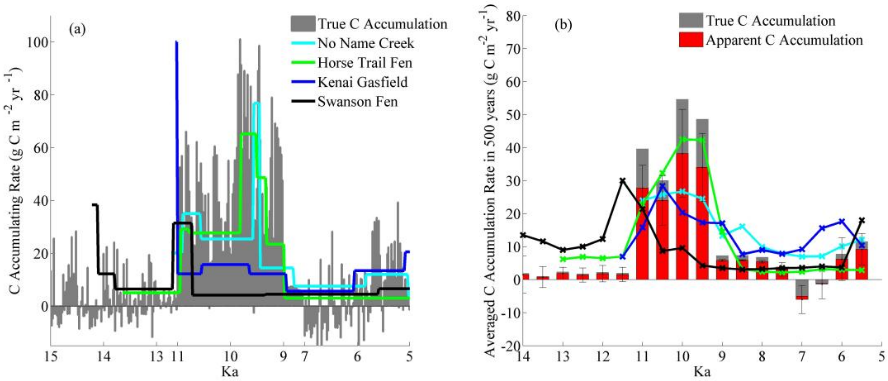

Figure 4. Simulated and observed carbon accumulation rates from 15 ka to 5 ka in 20-yr bins (a) and 500-yr bins with standard deviation (b) for No Name Creek, Horse Trail Fen, Kenai Gasfield, and Swanson Fen. Peat-core data were from Jones and Yu (2010).

Biogeosciences Discuss., doi:10.5194/bg-2016-284, 2016
Manuscript under review for journal Biogeosciences
Published: 14 July 2016

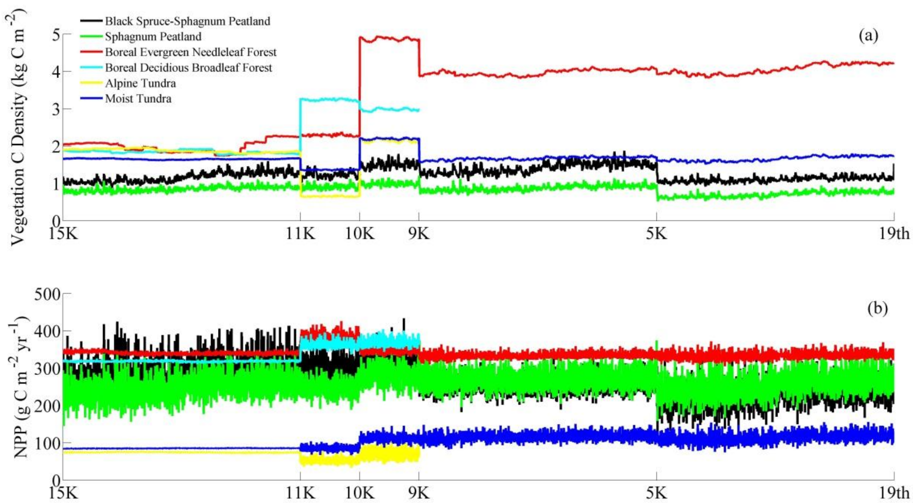

Figure 5. Simulated (a) mean vegetation carbon density (kg C m^{-2}) of different vegetation types and (b) NPP (g C $m^{-2}yr^{-1}$).

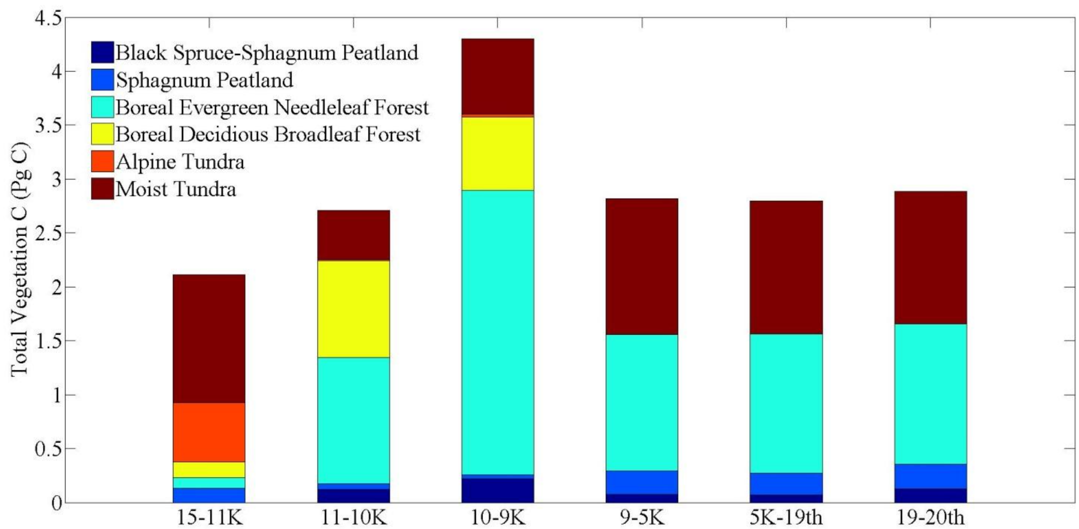

Figure 6. Total C (Pg C) stored in vegetation of Alaska for different time periods.

Biogeosciences Discuss., doi:10.5194/bg-2016-284, 2016
Manuscript under review for journal Biogeosciences
Published: 14 July 2016

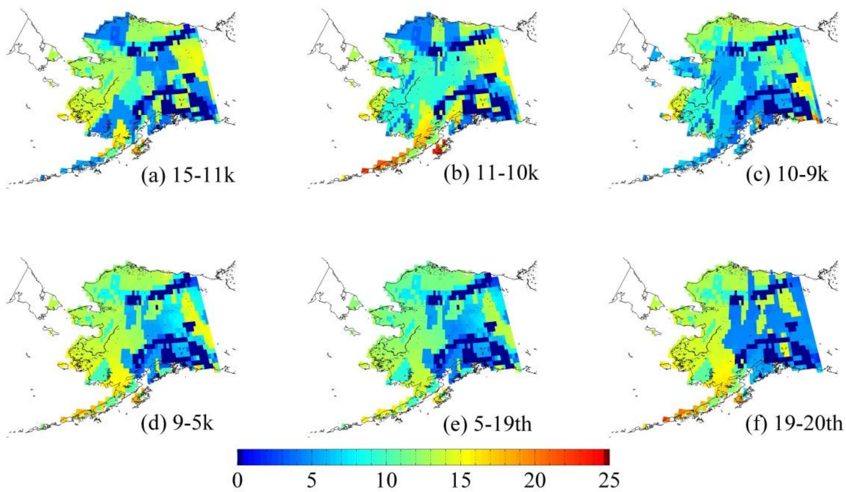

Figure 7. Non-peatland (mineral) SOC density (kg C m^{-2}) (cumulative) during (a) 15-11 ka, (b) 11-10 ka, (c) 10-9 ka, (d) 9-5 ka, (e) 5 ka -1900 AD, and (f) 1900-2000 AD.

Biogeosciences Discuss., doi:10.5194/bg-2016-284, 2016
Manuscript under review for journal Biogeosciences
Published: 14 July 2016

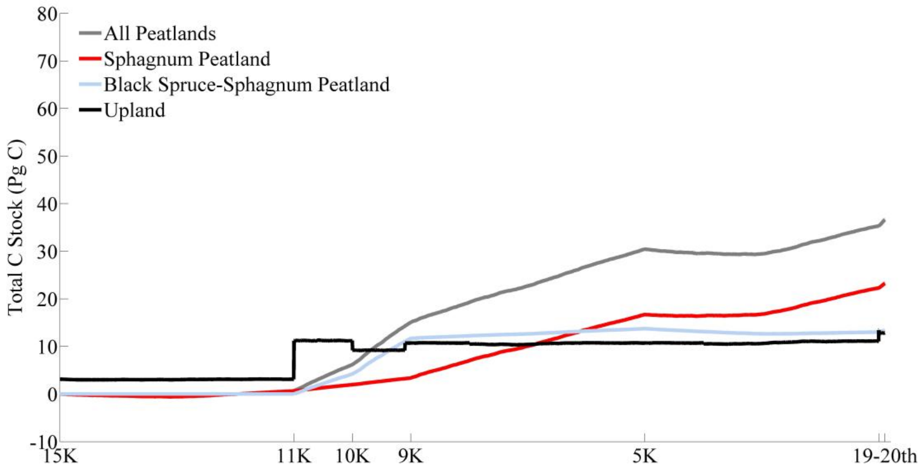

Figure 8. Total C stock accumulated from 15 ka to 2000 AD for all peatlands, *Sphagnum* open peatland, *Sphagnum*-black spruce peatland, and upland soils.

Biogeosciences Discuss., doi:10.5194/bg-2016-284, 2016
Manuscript under review for journal Biogeosciences
Published: 14 July 2016

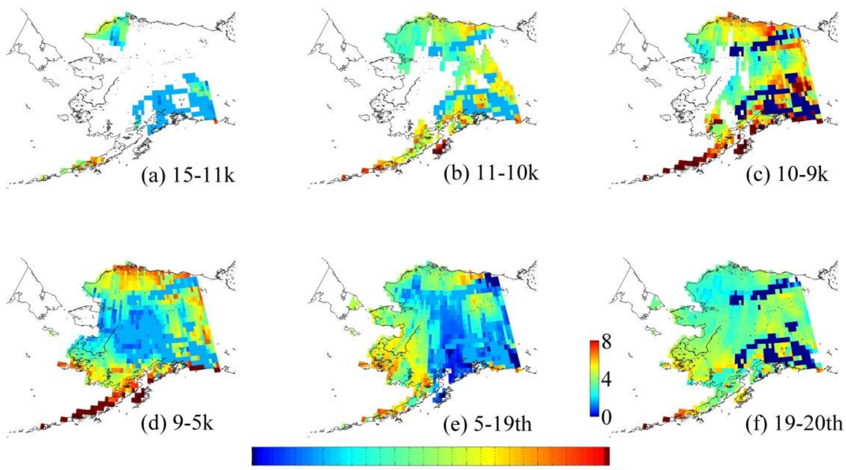

974
975 Figure 9. Peatland area expansion and peat soil C accumulation per 1000 years (kg C m^{-2} kyr^{-1})
976 during (a) 15-11 ka, (b) 11-10 ka, (c) 10-9 ka, (d) 9-5 ka, (e) 5 ka -1900 AD, and (f) 1900-2000
977 AD. The amount of C represents the C accumulation as the difference between the peat C
978 amount in the final year and the first year in each time slice.

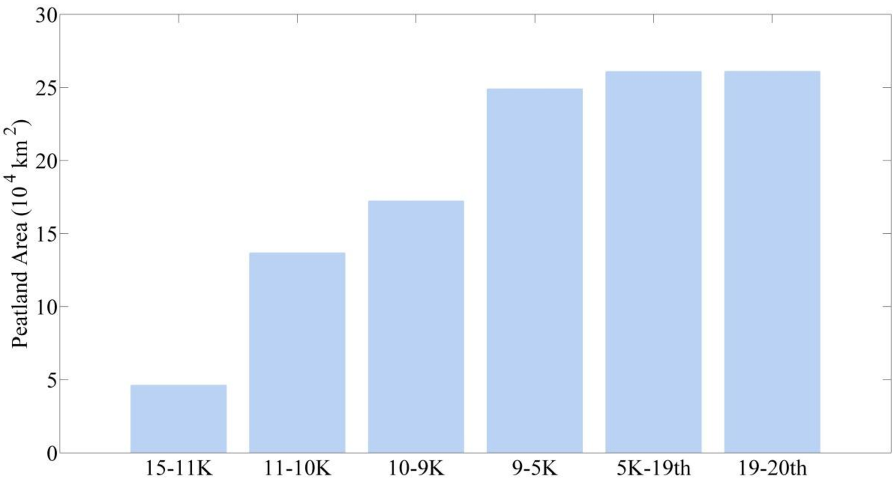

Figure 10. Peatland expansion area (10^4 km^2) in different time slices, the area of barren in the map is set to 0 km^2.

Biogeosciences Discuss., doi:10.5194/bg-2016-284, 2016
Manuscript under review for journal Biogeosciences
Published: 14 July 2016

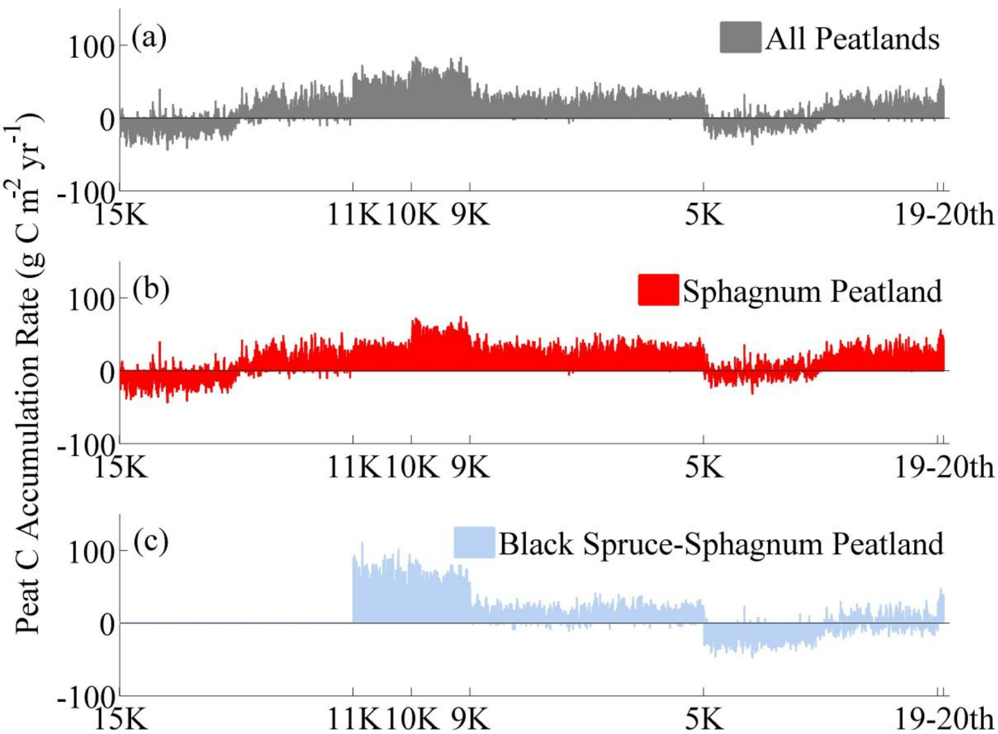

997

998 Figure 11. Peatland mean C accumulation rates from 15 ka to 2000 AD for (a) weighted average
999 of all peatlands, (b) *Sphagnum* open peatland, and (c) *Sphagnum*-black spruce peatland.

Biogeosciences Discuss., doi:10.5194/bg-2016-284, 2016
Manuscript under review for journal Biogeosciences
Published: 14 July 2016

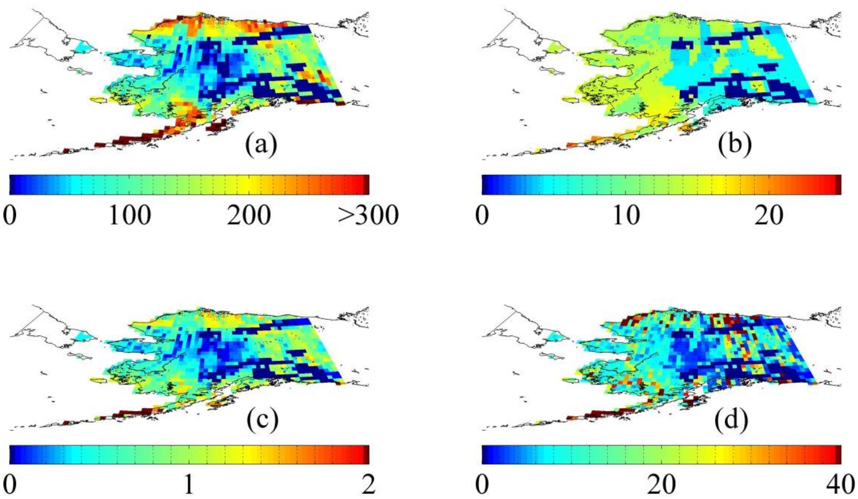

Figure 12. The spatial distribution of (a) total peat SOC density (kg C m^{-2}), (b) total mineral SOC density (kg C m^{-2}), (c) total peat depth (m), and (d) weighted average of total (peatlands plus non-peatlands) SOC density (kg C m^{-2}) in Alaska from 15 ka to 2000 AD.

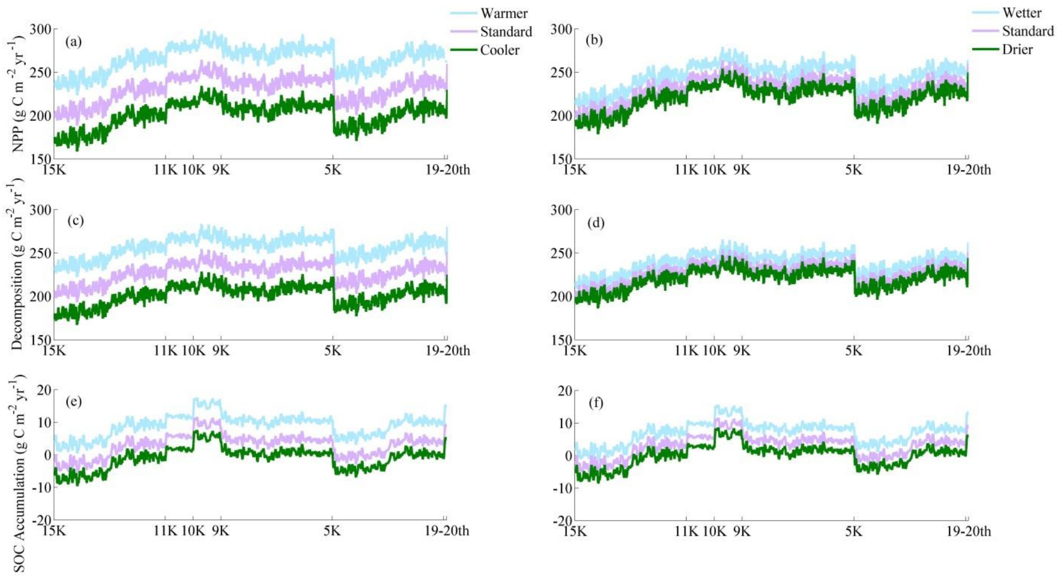

1016

Figure 13. Temperature and precipitation effects on (a)(b) annual NPP, (c)(d) annual SOC decomposition rate (aerobic plus anaerobic), and (e)(f) annual SOC accumulation rate of Alaska. A 10-year moving average was applied.

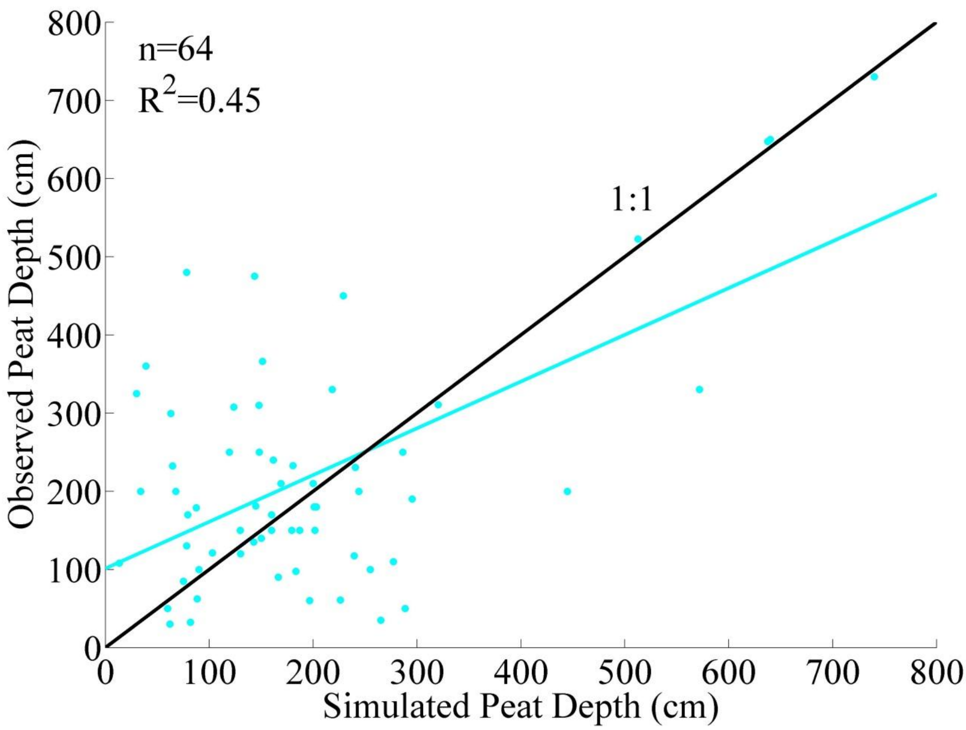

Figure 14. Field-based estimates and model simulations for peat depths in Alaska: The observed and simulated data are extracted from the same grids on the map. Linear regression line (cyan) is compared with the 1:1 line. The linear regression is significant ($P<0.001$, $n = 64$) with $R^2 = 0.45$, slope = 0.65, and intercept = 101.05 cm. The observations of >1000 cm are treated as outliers.